Journal of Nuclear Materials 467 (2015) 457–464

Contents lists available at ScienceDirect

Journal of Nuclear Materials

journal homepage: www.elsevier.com/locate/jnucmat

Statistical study of defects caused by primary knock-on atoms in fcc Cu and bcc W using molecular dynamics

M. Warrier [a, *], U. Bhardwaj [a], H. Hemani [a], R. Schneider [b], A. Mutzke [c], M.C. Valsakumar [d]

[a] Computational Analysis Division, BARC, Visakhapatnam, Andhra Pradesh, 530012, India
[b] Computational Science, Ernst-Moritz-Arndt University, D-17489 Greifswald, Germany
[c] Max-Planck-Institut für Plasmaphysik, D-17491 Greifswald, Germany
[d] School for Engineering Sciences and Technology, University of Hyderabad, Gachibowli, Hyderabad, Telangana State, 500046, India

HIGHLIGHTS

- MD simulations of collision cascades in 200 random directions explored in the energy range of 1–5 keV for fcc Cu and bcc W.
- 60–80 random directions must be sampled for the number of displacements produced in a collision cascade to stabilize.
- In-cascade clustering of interstitials and vacancies occur.
- Direction averaged distribution of interstitials and vacancies around the origin of a PKA is presented.
- Comparisons with MD indicate that the recoils produced in BCA-MC simulations be checked for recombination against all vacancies created.

GRAPHICAL ABSTRACT

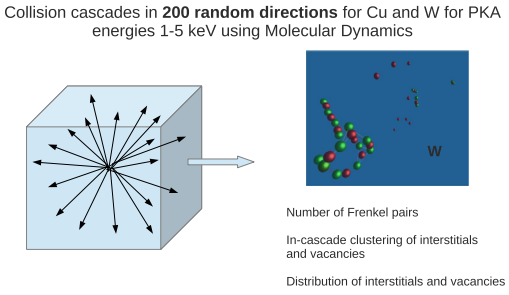

ARTICLE INFO

Article history:
Received 12 February 2015
Received in revised form
9 September 2015
Accepted 14 September 2015
Available online 16 September 2015

Keywords:
Irradiation
Cascade damage
Molecular dynamics
BCA Monte Carlo
PKA

ABSTRACT

We report on molecular Dynamics (MD) simulations carried out in fcc Cu and bcc W using the Large-scale Atomic/Molecular Massively Parallel Simulator (LAMMPS) code to study (i) the statistical variations in the number of interstitials and vacancies produced by energetic primary knock-on atoms (PKA) (0.1–5 keV) directed in random directions and (ii) the in-cascade cluster size distributions. It is seen that around 60–80 random directions have to be explored for the average number of displaced atoms to become steady in the case of fcc Cu, whereas for bcc W around 50–60 random directions need to be explored. The number of Frenkel pairs produced in the MD simulations are compared with that from the Binary Collision Approximation Monte Carlo (BCA-MC) code SDTRIM-SP and the results from the NRT model. It is seen that a proper choice of the damage energy, i.e. the energy required to create a stable interstitial, is essential for the BCA-MC results to match the MD results. On the computational front it is seen that in-situ processing saves the need to input/output (I/O) atomic position data of several terabytes when exploring a large number of random directions and there is no difference in run-time because the extra run-time in processing data is offset by the time saved in I/O.

* Corresponding author.
E-mail address: Manoj.Warrier@gmail.com (M. Warrier).

http://dx.doi.org/10.1016/j.jnucmat.2015.09.025
0022-3115/

1. Introduction

Primary damage of materials due to neutron irradiation occurs via energetic cascades caused by energetic primary knock-on atoms (PKA) created by energetic neutrons as they pass through the material. These cascades result in creation of Frenkel Pairs (interstitial–vacancy pairs). The interstitials and vacancies diffuse to (I) nullify the damage when an interstitial recombines with a vacancy, (II) form interstitial clusters when two or more interstitials recombine, and (III) form vacancy clusters when several vacancies come together. The long term changes in micro-structure and composition of the irradiated material is a multi-scale problem [1–5].

The primary cascades are modeled either by Molecular Dynamics ([1] and references therein) or by binary collision approximation (BCA) Monte Carlo Simulations [6–9]. The BCA breaks down only in the eV range when many body collisions become important [6]. In the BCA there is ambiguity in identifying a displaced atom. An atom is considered to be displaced in either of two ways: (1) if it has an energy greater than a specified displacement energy E_d, i.e., the threshold energy that an atom needs to be a stable interstitial [6,9], or (2) if it is at a distance greater than a specified distance from a vacancy, called the vacancy recapture radius. This vacancy recapture radius is obtained from considerations of crystal mechanical stability [10] and varying criteria are used ($2.5\,a_0$ in Refs. [7] and $1.36\,a_0$ in Refs. [8], where a_0 is the lattice parameter of the target material). There is also ambiguity in the value of the displacement energy E_d, [6,11–13].

MD simulations of collisional cascades takes into consideration many body effects and therefore is more accurate than simulations using BCA Monte Carlo codes [14]. MD also provides insight into the atomistic details like in-cascade clustering of interstitials, their configuration and also their dynamic evolution up-to several nanoseconds. However, MD has inherent limitations in the number of atoms it can simulate (at most a hundred billion atoms, which corresponds to a metallic solid of size equal to a fraction of a micron, on advanced supercomputers), the time it can span (around 10 ns) and the huge computational costs involved. MD simulations of collision cascades seldom account for electronic stopping losses. Special procedures have to be introduced in MD codes to take this into account [15,16].

Bacon et al., have studied the effect of collision cascades in fcc, bcc and hcp metals [17,18]. They showed that the in-cascade clustering of self–interstitials and vacancies occur in all metals and the clustering varies from metal to metal. Fikar et al. [19], have carried out MD studies of collision cascades in W in the 1–50 keV range using two different EAM potentials stiffened by two different repulsive potentials for short range interactions. They used two different random seeds to initialize the velocities of the atoms and chose three different directions (⟨135⟩, ⟨235⟩ and ⟨122⟩) to obtain statistical averages. Caturla et al. [20], have carried out a comparative study of radiation damage in Fe and Cu and have used the spatially correlated locations of vacancy and interstitials, obtained from MD simulations as inputs to a kinetic Monte Carlo (KMC) code to obtain defect clusters. At the end of the collision cascade in MD they see different cluster size distributions in Cu as compared with Fe. Becquart et al., have shown the effect of internal structure of displacement cascades and, in particular of self interstitial atom (SIA) agglomeration, on the long–term evolution of defect cluster growth [21]. Stoller et al., have carried out several hundred MD simulations along the ⟨100⟩, ⟨110⟩, ⟨111⟩ and ⟨135⟩ directions of Fe in the energy range from 0.1 to 50 keV, to statistically analyze MD cascades in bcc iron at 100 K [14]. Randomness was introduced in their simulations by carrying out NPT simulations to equilibrate the target to different times, choosing a different PKA location, or a combination of both. More recently Warrier et al., carried out MD simulations of PKAs directed along 1000 random directions in Fe (90%)–Cr (10%) alloy in the energy range of 0.1–5 keV [22]. They showed that at least a hundred random directions have to be explored for the standard deviation in the number of displaced atoms to stabilize.

In this study, we direct the PKA in 200 random directions for bcc W and fcc Cu in the energy range of 1–5 keV. We obtain direction averaged values of (i) number of interstitials and vacancies (hitherto referred to as displacements), (ii) clustering of displacements, (iii) range of PKA and (iv) distribution of displacements around the point of origin of PKA, for the 200 random directions. We compare the results from MD simulations with the BCA-MC code SDTRIM-SP [9] and the NRT model [10]. In the next section we describe the simulations and methods used. Then results from the MD simulations on number of Frenkel pairs, their distribution and clustering are presented in Section.3. In Section.4 the results from the BCA-MC code are compared with the MD results. Finally we present the conclusions from the study.

2. Description of the simulations and methods

Cascade simulations were carried out with both MD and BCA-MC codes. The Large-scale Atomic/Molecular Massively Parallel Simulator (LAMMPS) code [23], was used to carry out the MD simulations. Table 1 and Table 2 show the size of the cubic simulation box used for the Cu and W simulations in the second column and number of directions explored in the third column, along with other direction averaged results described in the results section. The PKA is a lattice atom lying at the center of the cubic box. For Cu and W, 200 MD simulations of the PKA in random directions at energies of 1, 2, 3, 4, and 5 keV respectively were carried out. At each energy, a new seed for the random number generator is used to obtain the 200 random directions thereby making the sequence of directions explored unique.

The embedded atom potential (EAM) developed by Sabochick and Lam [24] and stiffened by Nordlund et al. [25] to simulate the

Table 1
Statistical data for cascades in Cu: Here N_{disp} is the average number of interstitial–vacancy pairs, *nx*, *ny*, *nz* are the number of unit cells of size 3.615 Å used in the simulation, sample size is the number of directions sampled, PKAD is the average range of PKAs, and MaxR - the average maximum range in a cascade. The values after the ± sign are the standard deviations of these quantities.

E_{PKA} (keV)	nx = ny = nz	Sample size	N_{disp}	*PKAD* (Å)	*MaxR* (Å)
1	60	200	4 ± 1	11.6 ± 5.0	12.9 ± 4.1
2	80	200	6 ± 2	18.2 ± 10.1	20.9 ± 9.1
3	100	200	8 ± 3	24.3 ± 14.8	27.4 ± 13.2
4	110	200	9 ± 4	31.3 ± 20.6	36.6 ± 20.0
5	110	200	11 ± 4	37.1 ± 26.4	43.0 ± 25.2

Table 2
Statistical data for cascades in W: Here N_{disp} is the average number of interstitial–vacancy pairs, *nx*, *ny*, *nz* are the number of unit cells of size 3.157 Å used in the simulation, sample size is the number of directions sampled, PKAD is the average range of PKAs, and MaxR - the average maximum range in a cascade. The values after the ± sign are the standard deviations of these quantities.

E_{PKA} (keV)	nx = ny = nz	Sample size	N_{disp}	*PKAD* (Å)	*MaxR* (Å)
1	50	200	3 ± 1	8.3 ± 3.1	9.51 ± 2.3
2	50	200	5 ± 2	11.7 ± 4.4	13.4 ± 3.5
3	50	200	7 ± 2	12.9 ± 6.6	16.3 ± 5.6
4	50	200	9 ± 2	15.7 ± 7.6	19.3 ± 7.0
5	50	200	10 ± 3	20.7 ± 13.9	25.1 ± 12.7

repulsive part of atomic interactions correctly, was used for the Cu simulations. For W, the EAM/alloy potential implemented by G. Ziegenhain based on the method by Zhou et al. [26] was used. The pair part of this potential was stiffened [27] by connecting it smoothly using cubic splines to the ZBL potential [28] at inter–atomic separations less than 1.2 Å. It was verified that the modified potential reproduces the lattice parameter (3.165 Å), cohesive energy (8.757 eV/atom) and vacancy formation energy (3.567 eV) of W correctly. Periodic boundary conditions are specified in all three directions and the atoms in the outermost unit cells on all faces of the cube are kept fixed. Scoping runs, using a Nosé-Hoover NPT ensemble at 300 K established that equilibrium was reached in 8–10 ps. It was also verified that the cascade dynamics in the energy range being explored saturates within 5 ps [22]. Adaptive time stepping was used with the criterion for the time step being decided by either a minimum time step of 0.01 fs or the time required by the fastest atom to move being 0.1 Å, whichever is smaller. The cascade simulations were then run for 6 ps using a micro–canonical ensemble.

For the BCA-MC simulations, the SDTRIM-SP code [9] was used to simulate the PKA cascades in the same energy range as that of the MD simulations. For comparison with MD results and with the NRT model, the following cases were explored in the SDTRIM-SP simulations:

(1). Electronic stopping was switched off, since the MD simulations do not take this into consideration.
(2). Electronic stopping is switched on. SDTRIM-SP simulations with the default value of E_d in SDTRIM-SP (38 eV for W, and 19 eV for Cu) are carried out.
(3). Electronic stopping was on and E_d of 40 eV for Cu (to match the NRT standard) was used. For W, a value of E_d from MD calculations [13], 98 eV, was used since the default value in SDTRIM-SP is close to the NRT standard of 40 eV. Moreover it is interesting to see how a MD derived value for E_d used in a BCA-MC code compared with the MD results.

The displacement energy E_d was fixed at 40 eV for Cu and W in the NRT model.

The procedure for finding the surviving number of Frenkel Pairs has been described in Ref. [22]. Essentially, the distance between the initial position (perfect lattice site) and the current positions of each atom is monitored and if it is greater than a specified value (r_{disp}), it is considered to be displaced. The distance between each of the displaced atoms and vacancy sites (initial positions of the displaced atoms) are then calculated. If this distance is less than a specified value (r_{rec}) for a displaced atom–vacancy pair, the displaced atom is considered to have occupied the vacant lattice site. In our simulations we take $r_{disp} = r_{rec} = 0.3a$, where a is the lattice constant. We have verified that this choice nicely separates the interstitial offsets from the offsets of crystal atomic positions due to thermal vibrations, by carrying out NRT MD simulations of a single interstitial in a $10 \times 10 \times 10$ unit cell crystal of Cu and W at 300 K. The surviving displaced atoms that do not recombine with a vacancy are then analyzed to see if they are dumbbells or crowdions and the correct number of displaced atoms is calculated [1]. The range of the PKA and the maximum displacement of the recoils (displaced atoms) are also monitored.

2.1. Correcting the displaced atoms for crowdions and dumbbells; clustering defects

We use Union-Find or disjoint-sets data structure [29] to group the defects that are closer than 1-NN (nearest neighbor). The algorithm is as follows:

(1). Initiate a union-find data-structure with every defect as the only member of its own group.
(2). If the distance between any two defects is less than the specified threshold, then union their groups.
(3). Tag each defect with the group it belongs to.

The above grouping will have an over–counting of defects due to appearance of an interstitial as two interstitials and one vacancy in a dumbbell configuration or three interstitials and two vacancies in a crowdion configuration or similar appearances in complex clusters. We then account for the over–counting as follows:

(1). Label all vacancies as −1 and all interstitials as 1.
(2). Add all the labels.
(3). The absolute of resulting number is the corrected number of defects in that cluster.
(4). If the resulting number is greater than zero then the defects in the cluster are of type interstitials, if it is less than zero then it is of type vacancy. If resulting number equals zero then there are no defects in the group.

Although, we have now obtained the number of defects after accounting for dumbbells and crowdions, we need the co-ordinates of the surviving defects for cluster size distribution. For this we annihilate the vacancy–interstitial pairs in a group which are closest. The algorithm to do this in each group is as follows:

(1). Find the type of group (interstitial/vacancy) from the above algorithm.
(2). For every species that is not same as the group type, find the closest pair of the other species.
(3). Mark both defects in the pair as deleted from the group.

Using the corrected defect coordinates, we find the distribution of their distances from the PKA. We again use the Union-Find data structure based grouping algorithm described above on surviving defects' coordinates to get the cluster size-distribution of interstitials and vacancies.

3. Results from the MD simulations

The evolution of the number of displacements as a function of time for Cu and W are shown for a random PKA at each of the energy ranges explored in Fig. 1 and Fig. 2 respectively. It is seen

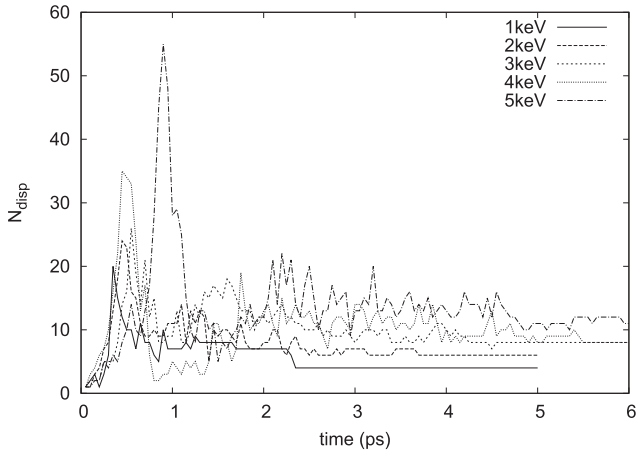

Fig. 1. Total number of displacements as a function of time for Cu PKA at energy 1,2,3,4 and 5 keV.

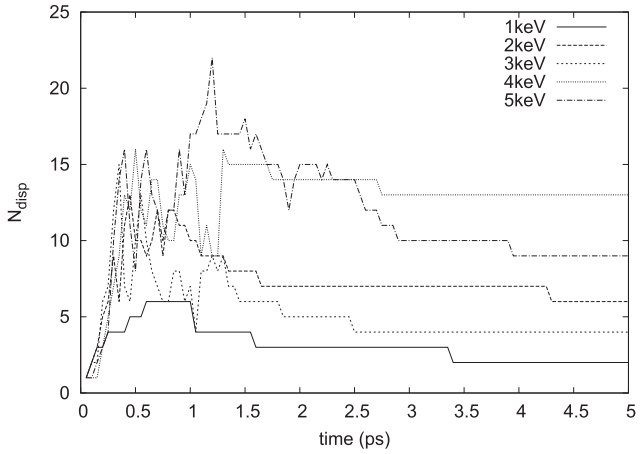

Fig. 2. Total number of displacements as a function of time for W PKA at energy 1,2,3,4 and 5 keV.

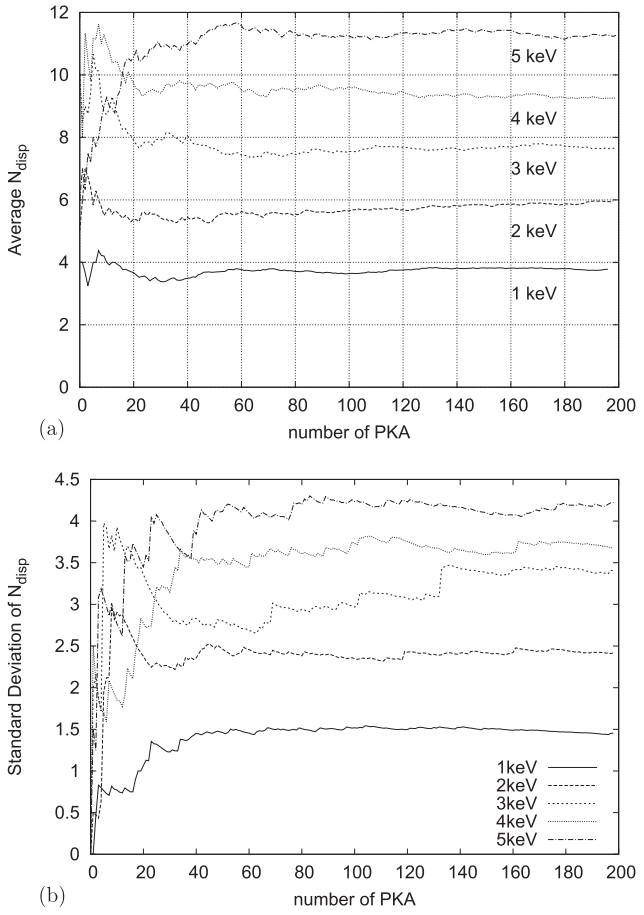

Fig. 3. Variation of (a) the number of displacements, and (b) standard deviation of the number of displacements, in Cu as a function of the number of the PKAs launched in random directions at energies 1–5 keV.

that the time scales for the collision cascade dynamics is a few ps and the number of displacements saturate by 6 ps. At lower PKA energy, the saturation occurs faster. Note that these displacements have been corrected for over-counting due to dumbbell and crowdion configurations at each time step. We note that if these corrections are not applied, there are several hundreds of displacements appearing transiently during the peak of the cascade.

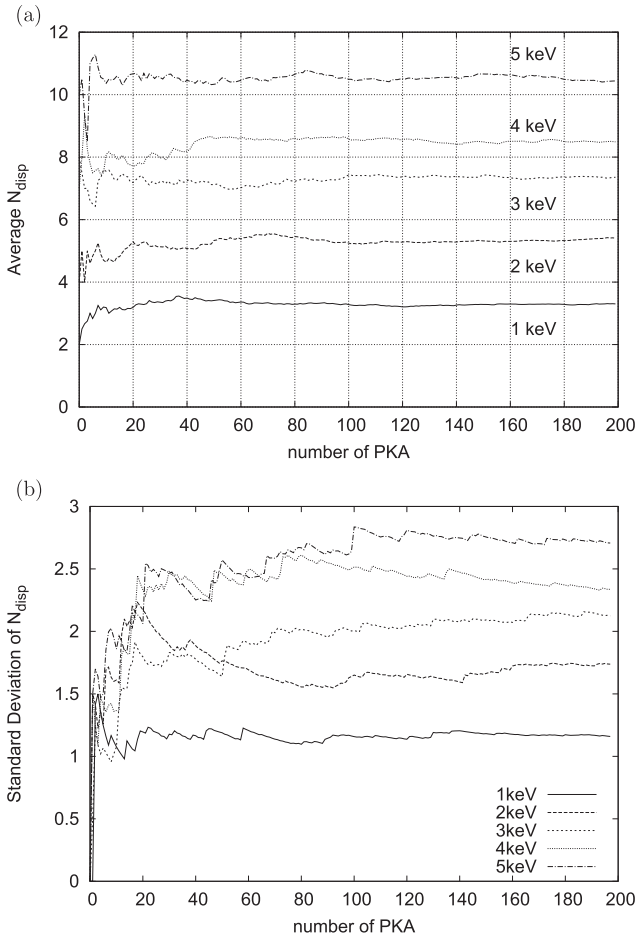

Fig. 4. Variation of (a) the number of displacements, and (b) standard deviation of the number of displacements, in W as a function of the number of the PKAs launched in random directions at energies 1–5 keV.

Tables 1 and 2 shows the average number of displacements, the average range of the PKA, the average range of the maximum displacement and the variance of these parameters over the 200 random directions sampled.

The average number of displacements $n_{avg,N}$ for N PKA directions simulated is given by

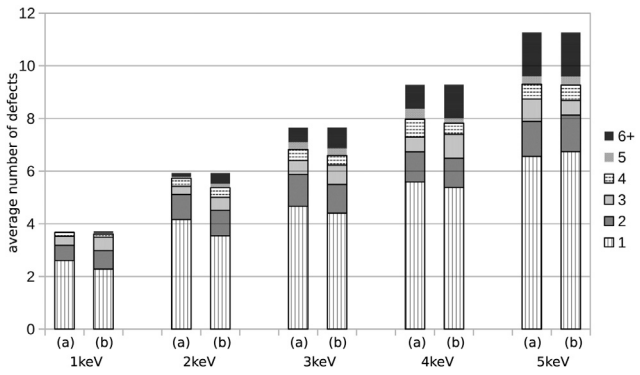

Fig. 5. Bar-plot of the (a) interstitial and (b) vacancy, cluster size distributions in Cu for PKA energies of 1–5 keV, averaged over the 200 random directions.

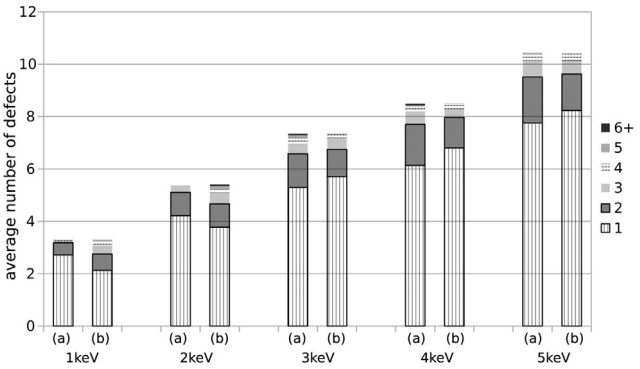

Fig. 6. Bar-plot of the (a) interstitial and (b) vacancy, cluster size distributions in W for PKA energies of 1–5 keV, averaged over the 200 random directions.

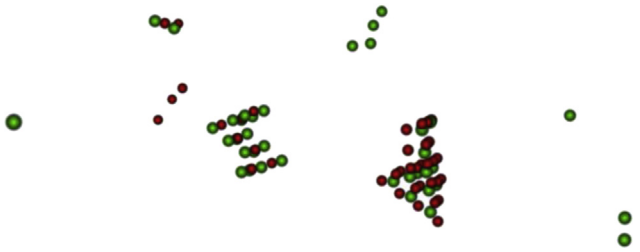

Fig. 7. A picture of the Frenkel pairs in Cu at PKA energy of 5 keV. Vacancies are in red and the interstitials are in green color. Note that dumbbells and bunched clusters are common in Cu. (For interpretation of the references to color in this figure legend, the reader is referred to the web version of this article.)

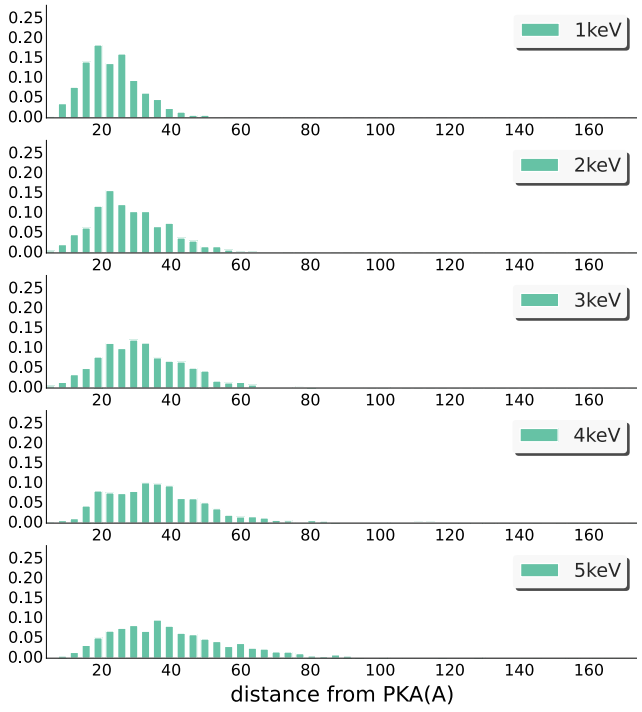

Fig. 9. Distribution of the interstitials as a function of distance from the origin of the PKA for energies 1–5 keV in Cu.

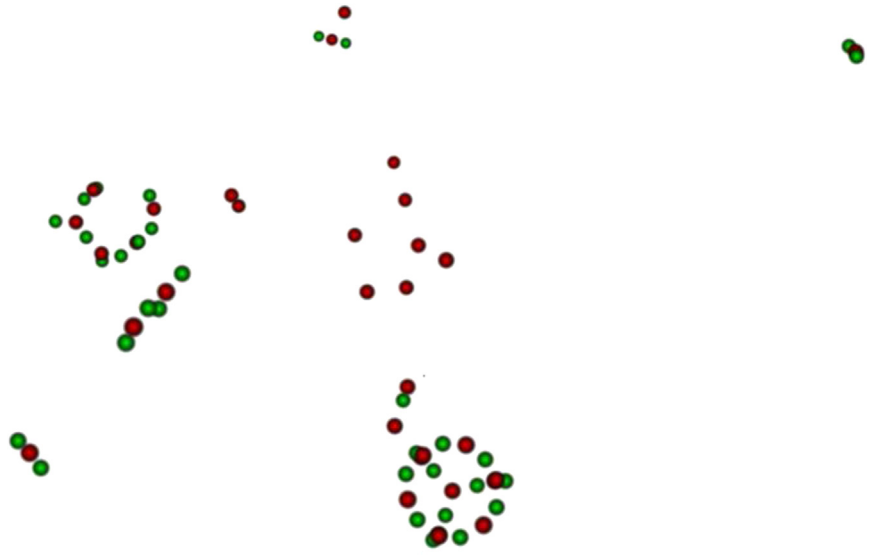

Fig. 8. A picture of the Frenkel pairs in W at PKA energy of 5 keV. Vacancies are in red and the interstitials are in green color. It shows dumbbells, crowdions and ring like arrangement of interstitial clusters. (For interpretation of the references to color in this figure legend, the reader is referred to the web version of this article.)

$$n_{avg,N} = \sum_{i=1}^{N} \frac{n_{d,i}}{N}$$

where, $n_{d,i}$ is the number of displacements in the ith PKA direction. The standard deviation in the number of displacements for N PKA directions σ_N is given by

$$\sigma_N = \left(\sum_{i=1}^{N} \frac{(n_{d,i} - n_{avg,N})^2}{N} \right)^{1/2}$$

For the Cu simulations, a plot of $n_{avg,N}$ and σ_N as a function of N is shown in Fig. 3 (a) and (b) respectively. For W, the plot of $n_{avg,N}$ and σ_N as a function of N is shown in Fig. 4 (a) and (b) respectively. It is seen that around 60–80 random directions in fcc Cu, and around

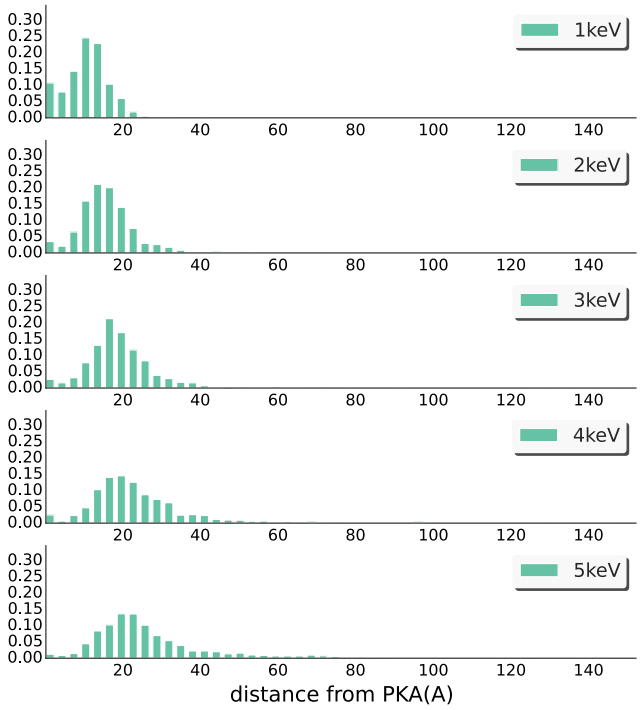

Fig. 10. Distribution of the Vacancies as a function of distance from the origin of the PKA for energies 1–5 keV in Cu.

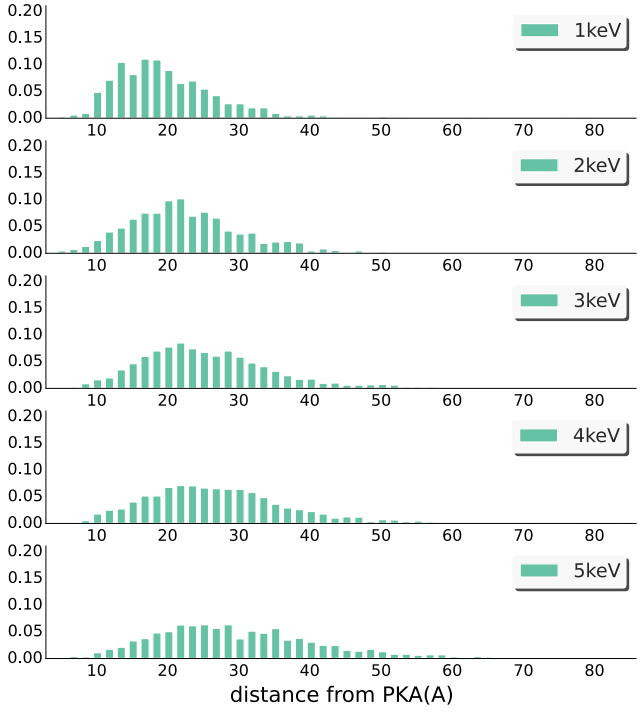

Fig. 11. Distribution of the interstitials as a function of distance from the origin of the PKA for energies 1–5 keV in W.

50–60 random directions in bcc W, have to be sampled for the average number of displaced atoms ($n_{avg,N}$) to stabilize. However for σ_N to stabilize, 100–150 random directions in Cu and around 100 random directions in W have to be sampled.

The cluster size distributions of interstitials and vacancies for

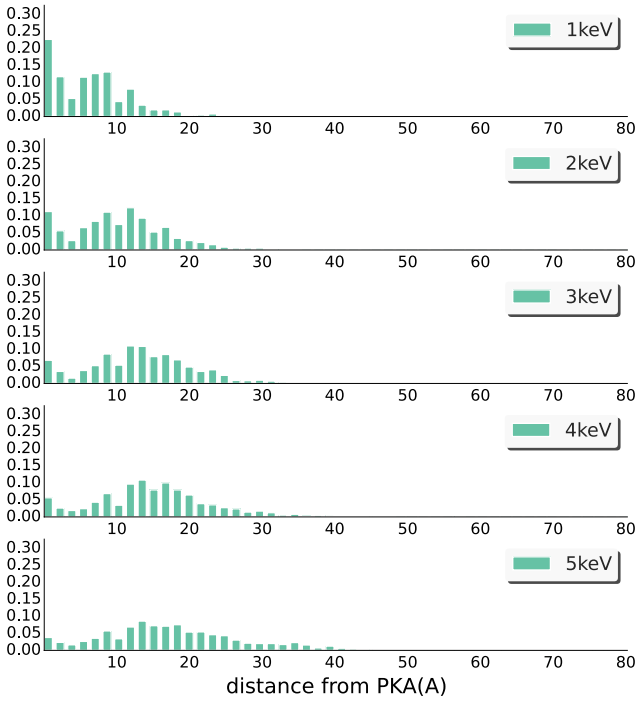

Fig. 12. Distribution of the Vacancies as a function of distance from the origin of the PKA for energies 1–5 keV in W.

Cu and W averaged over the 200 random directions at each of the PKA energies explored are presented in Fig. 5, and Fig. 6 respectively. These are stacked bar plots, where the shaded area under each bar corresponds to the number of interstitial/vacancy clusters of specified size. From this it is clear that in-cascade clustering of both vacancies and interstitials occur, but most of the interstitials and vacancies are single for both Cu and W. This is at odds with the results presented in Ref. [17] where more that half the interstitials are in clusters of size two or more for cascades in Cu carried out at 100 K for PKA energies 2–5 keV. The difference in results could be either due to the difference in temperatures or more probably, due to the different interaction potentials used in the simulations. Note that cascades in Cu show more clusters of five or more defects, even at relatively low PKA energies, as compared to W.

Dumbbells and crowdions are observed for both, Cu and W, as shown in Fig. 7 and Fig. 8 respectively. Fig. 7 is for a 5 keV PKA in Cu and Fig. 8 is for a 5 keV PKA in W. Ring shaped clusters are seen in W and are few in number as compared to Cu which has bunched clusters as seen in the figure. The single interstitials and vacancies are more separated out in Cu as compared to W.

The direction averaged distribution of interstitials and vacancies around a PKA location for Cu and W are shown in Fig. 9, Fig. 10, Fig. 11 and Fig. 12 respectively. It is seen that the spread in both, interstitials and vacancies, increases with energy of PKA. The peak of the distributions also shift away from the origin of the PKA at higher PKA energies. Note that the spread in the interstitial distribution is slightly larger than that of the vacancies in both cases. The vacancies show a spike at the origin of the PKA due to the vacancy created as a result of PKA creation. These distributions are useful inputs for Object Kinetic Monte Carlo (OKMC) or Mean Field Rate Theory (MFRT) simulations [30] to model point defect cluster dynamics at length and time–scales not amenable to MD simulations.

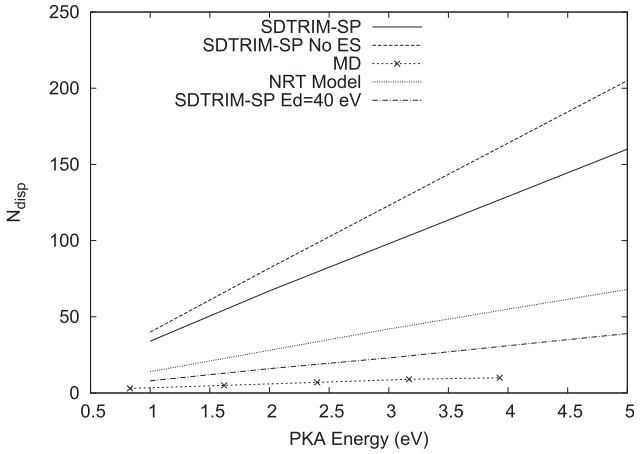

Fig. 13. Variation of the number of Frenkel Pairs as a function of the energy of PKA from MD simulations, NRT Model and SDTRIM-SP simulations for the three cases, viz. without electronic stopping, with electronic stopping, with $E_d = 40$ eV for Cu.

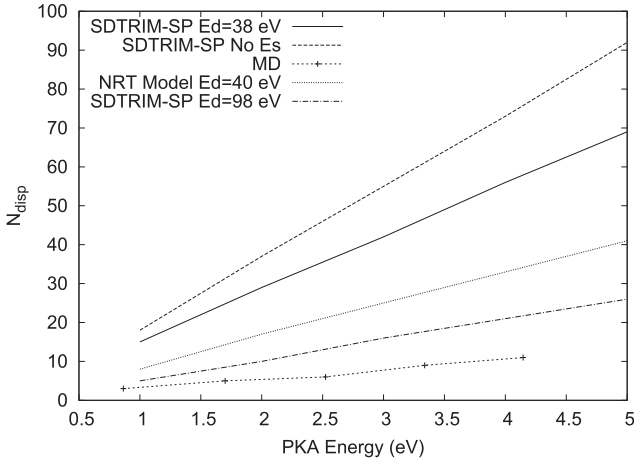

Fig. 14. Variation of the number of Frenkel Pairs as a function of the energy of PKA from MD simulations, NRT Model and SDTRIM-SP simulations for the three cases, viz. without electronic stopping, with electronic stopping, with $E_d = 98$ eV for W.

4. Comparison of MD results with BCA-MC

Fig. 13 and Fig. 14 compares the surviving number of defects from our MD simulations for Cu and W respectively with the three cases for which the BCA-MC simulations were carried out and with the prediction from the NRT formula [10] (which uses $E_d = 40$ eV). The standard-value of E_d in SDTRIM-SP for Cu is 19 eV. For W, the value of E_d in SDTRIM-SP is 38 eV, which is close to the NRT value. Despite this, the results for the number of displaced atoms predicted by SDTRIM-SP is much higher than that from the MD simulations and the predictions of the NRT model for W. Therefore for W we use a value of E_d obtained from the MD studies of Setyawan et al. [13] and get a much closer match between the BCA-MC and MD simulations. For Cu, using a value of $E_d = 40$ eV, gives the closest match with the MD results, but is still higher than the MD results. Note that the PKA energies for the MD simulation results are the corrected values which take into account losses due to electronic stopping as recommended in Ref. [1].

The BCA-MC results show a much higher number of displaced atoms than that predicted by MD and do not match the MD results unless a higher value of E_d is chosen. By definition, E_d is the energy required to create a stable Frenkel pair. In the context of an isolated defect, it is the energy required to permanently displace an atom from its equilibrium position thereby creating an interstitial and a vacancy which cannot recombine. In the context of radiation damage, there is a possibility of the interstitial obtained by displacing an atom annihilating with some other vacancy created by the cascade. This is not taken into consideration in the SDTRIM-SP simulations.

Therefore, in BCA-MC simulations E_d is a crucial parameter that influences the number of displacements created. It is recommended that in BCA-MC codes, final recoil positions be tested for stability with other vacancy sites created in the cascade by specifying a vacancy recapture radius. This recommendation has not been proved in this paper, but it seems desirable to account for the recombination of interstitials with vacancies other than its original vacancy.

5. Conclusions

Using molecular dynamics simulations, we show that collision cascades caused by PKA in the energy range 1–5 keV, around 60–80 random directions of PKA in fcc Cu and around 50–60 random directions of PKA in bcc W, have to be sampled for the number of displacements produced to stabilize around an average value. The cluster size distributions of interstitials and vacancies averaged over the 200 random directions have been plotted. It is seen that most of the interstitials and vacancies created are single for both Cu and W and Cu has bigger cluster sizes than W. The direction averaged distribution of vacancies and interstitials around the starting point of a PKA is also shown for both, Cu and W in the PKA energy range 1–5 keV.

All these data are useful inputs to higher scale simulations of radiation damage. Similar collision cascade simulations were also carried out using the BCA-MC code SDTRIM-SP and the results were compared with MD simulations. It is seen that the BCA-MC results have a better match with the MD results when a value of the displacement energy, E_d, obtained from MD simulations is used in the BCA-MC simulations. It is recommended that in BCA-MC codes, final recoil positions be tested for stability with other vacancy sites created in the cascade by specifying a vacancy recapture radius.

Acknowledgments

We would like to thank N. Sakthivel and his team from the supercomputing center and A. Majalee, all from C.A.D, BARC-Visakhapatnam for the supercomputing cluster support. M. Warrier would like to thank K. Nordlund for the stiffened Cu potential.

References

[1] R.E. Stoller, Primary radiation damage formation, in: R.J.M. Konings (Ed.), Comprehensive Nuclear Materials, vol. 1, 2012, pp. 293–332. Elsevier, 1.
[2] R.E. Stoller, L.K. Mansur, ORNL Report ORNL/TM-2005/506, 2005.
[3] P.R. Monasterio, B.D. Wirth, G.R. Odette, J. Nucl. Mater. 361 (2007) 127–140.
[4] C. Björkas, K. Nordlund, M.J. Caturla, Phys. Rev. B 85 (2012) 024105.
[5] C.S. Becquart, C. Domain, L.O. Malerba, M. Hou, Nucl. Instrum. Methods B 228 (2005) 181–186.
[6] W. Eckstein, Computer Simulations of Ion-solid Interactions, Springer Series in Material Science 10i, Springer Verlag, 1991.
[7] M.T. Robinson, I.M. Torrens, Phys. Rev. B 9 (1974) 5008–5024.
[8] J.R. Beeler Jr., Phys. Rev. 150 (1966) 470.
[9] A. Mutzke, R. Schneider, W. Eckstein, R. Dohmen, SDTrimSP Version 5.00, Max-Planck Institute for Plasmaphysics Report IPP 12/8, 2011.
[10] M.J. Norgett, M.T. Robinson, I.M. Torrens, Nucl. Eng. Des. 33 (1975) 50–54.
[11] K. Nordlund, J. Wallenius, L. Malerba, Nucl. Instrum. Methods B 246 (2006) 322–332.
[12] N. Juslin, K. Nordlund, J. Wallenius, L. Malerba, Nucl. Instrum. Methods B 255 (2007) 75–77.
[13] W. Setyawan, Aaron P. Selby, N. Juslin, Roger E. Stoller, Brian D. Wirth, Richard J. Kurtz, arxiv preprint, Condens. Matter Mater. Sci. (2014), 1412.7452v1.
[14] R.E. Stoller, A.F. Calder, J. Nucl. Mater. 283–287 (5) (2000) 746–752.

[15] A.M. Rutherford, D.M. Duffy, J. Phys. Condens. Matter 19 (2007) 496201.
[16] D.M. Duffy, A.M. Rutherford, J. Phys. Condens. Matter 19 (2007) 016207.
[17] D.J. Bacon, F. Gao, Yu N. Osetsky, J. Nucl. Mater. 276 (2000) 1–12.
[18] D.J. Bacon, Yu N. Osetsky, R. Stoller, R.E. Voskoboinikov, J. Nucl. Mater. 323 (2003) 152–162.
[19] Nucl. Instrum. Methods Phys. Res. B 255 (2007) 27–31.
[20] M.J. Caturla, N. Sonedab, E. Alonso, B.D. Wirth, T. Díaz de la Rubia, J.M. Perlado, J. Nucl. Mater. 276 (2000) 13–21.
[21] C.S. Becquart, C. Domain, L. Malerba, M. Hou, Nucl. Instrum. Methods Phys. Res. B 228 (2005) 181186.
[22] M. Warrier, M.C. Valsakumar, Fusion Sci. Technol. 65 (2) (2014) 222–228.
[23] S.J. Plimpton, J. Comput. Phys. 117 (1995) 1–19.
[24] M.J. Sabochick, N.Q. Lam, Phys. Rev. B 43 (1991) 5243.
[25] K. Nordlund, M. Ghaly, R.S. Averback, M. Chaturla, T. Diaz de la Rubia, J. Tarus, Phys. Rev. B 57 (1998) 7556.
[26] X.W. Zhou, H.N.G. Wadley, R.A. Johnson, D.J. Larson, et al., Acta Mater. 49 (19) (2001) 4005.
[27] C. Björkas, K. Nordlund, S. Dudarev, Nucl. Instrum. Methods Phys. Res. B 267 (2009) 3204.
[28] J.F. Ziegler, J.P. Biersack, U. Littmark, The Stopping and Range of Ions in Matter, Pergamon, New York, 1985.
[29] H. Thomas Cormen, Charles E. Leiserson, Ronald L. Rivest, Clifford Stein, “Chapter 21: Data Structures for Disjoint Sets”, Introduction to Algorithms (second ed.), MIT Press, p. 498524.
[30] R.E. Stoller, S.I. Golubov, C. Domain, C.S. Becquart, J. Nucl. Mater. 382 (2008) 77–90.